IASF/CNR
SEZIONE BOLOGNA
LFI Project System Team

Planck LFI

TITLE: # LFI 4π Beams at 30 GHz

DOC. TYPE: TECHNICAL NOTE

PROJECT REF.: PL-LFI-PST-TN-043 **PAGE:** I of V, 5

ISSUE/REV.: 1.0 **DATE:** July 2003

Prepared by	M. SANDRI F. VILLA LFI Project System Team	Date: Signature:	July 15th, 2003
Agreed by	C. BUTLER LFI Program Manager	Date: Signature:	July 15th, 2003
Approved by	N. MANDOLESI LFI Principal Investigator	Date: Signature:	July 15th, 2003

DISTRIBUTION LIST

Recipient	Company / Institute	E-mail address	Sent
M.BERSANELLI	Univ. Di Milano – Milano	bersanelli@uni.mi.astro.it	Yes
C.BURIGANA	IASF/CNR – Sezione di Bologna	burigana@bo.iasf.cnr.it	Yes
R.C.BUTLER	IASF/CNR – Sezione di Bologna	butler@bo.iasf.cnr.it	Yes
N.MANDOLESI	IASF/CNR – Sezione di Bologna	mandolesi@bo.iasf.cnr.it	Yes
A.MENNELLA	IASF/CNR – Sezione di Milano	daniele@mi.iasf.cnr.it	Yes
M.SANDRI	IASF/CNR – Sezione di Bologna	sandri@bo.iasf.cnr.it	Yes
J.TAUBER	ESA / ESTEC – Noordwijk	jtauber@rssd.esa.int	Yes
F.VILLA	IASF/CNR – Sezione di Bologna	villa@bo.iasf.cnr.it	Yes
F.PASIAN	OAT – Trieste	pasian@ts.astro.it	Yes
LFISPCC		lfispcc@bo.iasf.cnr.it	Yes

CHANGE RECORD

Issue	Date	Sheet	Description of Change	Release
1.0	July 2003	All	First issue of document	===

USEFUL ACRONYMS

Acronym	Description
GO	Geometrical Optics
GTD	Geometrical Theory of Diffraction
PO	Physical Optics
PTD	Physical Theory of Diffraction
MrGTD	Multi-reflector GTD
RDP	Reference Detector Plane
LOS	Line Of Sight
ET	Edge Taper

TABLE OF CONTENTS

1 INTRODUCTION

This note is to present the results of 4π beam optical simulations carried out for the LFI dual profiled corrugated feed horns at 30 GHz. Both polarizations have been considered for each feed. The simulations have been carried out in the transmitting mode using GRASP8 software package [1] coupled with the MrGTD add–on package [2]. In Section 2 the optical layout considered in the simulations is described. The 4π maps are reported in Section 3 whereas in Appendix some details of the simulation method are explained for completeness.

2 THE OPTICS

2.1 Telescope and shields

The PLANCK Telescope geometry is reported in [3], together with details of the coordinate systems defined to represent the telescope in GRASP8. The blocking structures considered in these simulations consist of the baffle and the upper V– groove, which is directly in view of the telescope and instrument. Fig. 1 shows the simulated optics (left and central panels) and the complete satellite geometry (right panel).

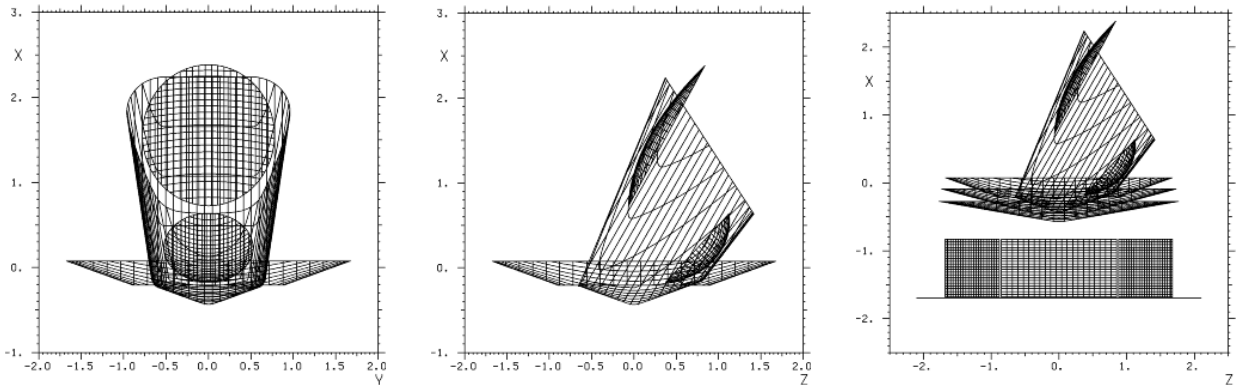

Fig. 1 Telescope and shields geometry in $(XY)_{TEL}$ (*left*) and $(XZ)_{TEL}$ (*centre*) planes; spacecraft geometry (*right*).

2.2 Focal Plane Layout

The location and orientation of the two LFI feed horns at 30 GHz are reported in Tab. 1, in the Reference Detector Plane Coordinate System [4]. The UV– location of the power peak of the corresponding beams on the sky are listed in Tab. 2, together with the orientation (with respect to the telescope line of sight) of the coordinate systems in which the beams have been computed [5]. The feed model used in the simulations is a Y– axis polarized dual profiled feed horn specified by its spherical wave expansion provided by Alcatel Space Industries, since the sub reflector is in the near field of the corrugated horn and near field effects cannot be neglected. The feed horn directivity is about 22 dBi and the ET is 30 dB at 22°. The X– axis polarized model has been obtained rotating each feed horn around its axis of 90 degrees.

Tab. 1 30 GHz LFI feed horn locations in the Focal Plane Unit (in the Reference Detector Plane coordinate system).

FH #	Location (X_{RDP},Y_{RDP},Z_{RDP}) [mm,mm,mm]			Orientation (θ_{RDP},φ_{RDP},ψ_{RDP}) [deg,deg,deg]		
27	-136.95	54.94	18.60	15.56	-23.01	-19.22
28	-136.95	-54.94	18.60	15.56	23.01	19.22

Tab. 2 Main beam locations on the sky ($u = \sin\theta \cdot \cos\varphi$, $v = \sin\theta \cdot \sin\varphi$) and polarization angle, ψ .

MB #	Location		Orientation (θ_{LOS},φ_{LOS},ψ_{LOS}) [deg,deg,deg]		
	U	V			
27	-0.06789	0.03369	4.3466	153.6074	-22.5000
28	-0.06789	-0.03369	4.3466	-153.6074	22.5000

3 4π BEAMS

Each beam has been computed in the co– and x– polar basis according to the Ludwig's third definition [6], in spherical polar cuts in which $\theta \in [-180°,+180°]$ and $\phi \in [0°,+178°]$, with $\Delta\theta = \Delta\phi = 2°$. The 4π maps are shown in Fig. 2 ÷ Fig. 5. In the left panel of each figure, the beam boresight direction is at the top of the map. Each polar cut with a constant ϕ value is a meridian of the map. The θ angle runs, on each meridian, from $\theta = 0°$ (towards the main beam direction) to $\theta = 180°$ (–180°) sweeping the map on its left (right) side. The ϕ angle goes from $\phi = 0°$ (centre of the map) to $\phi = 180°$ (left side of the map) on the left side of the map, and from $\phi = 0°$ (right side of the map) to $\theta \rightarrow 180°$ (centre of the map) on the right side of the map. Therefore the centre of the map has $\theta = 90°$ and $\phi = 0°$. Whereas in the right panel of each figure the main beam pointing direction is in the centre of the map, at $\theta = \phi = 0°$.

3.1 4π Beam #27

3.1.1 X– polarized

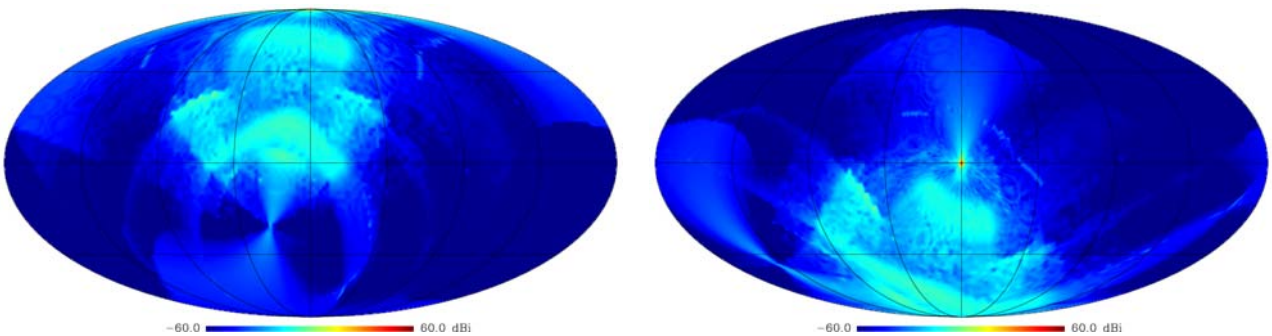

Fig. 2 Full Pattern of the LFI27 SWE X– axis polarized at 30 GHz (*power*). *Left:* the boresight direction is at the top of the map; *Right:* the boresight direction is in the centre of the map.

3.1.2 Y– polarized

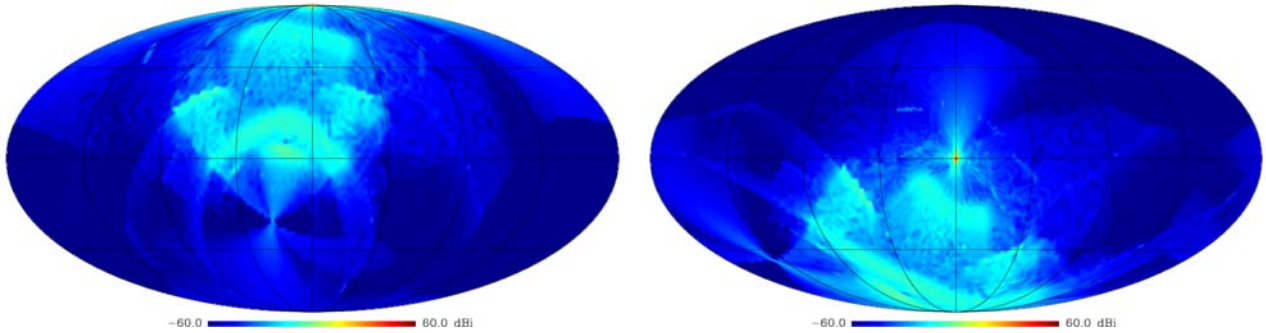

Fig. 3 Full Pattern of the LFI27 SWE Y– axis polarized at 30 GHz (power). *Left*: the boresight direction is at the top of the map; *Right*: the boresight direction is in the centre of the map.

3.2 4π Beam #28

3.2.1 X– polarized

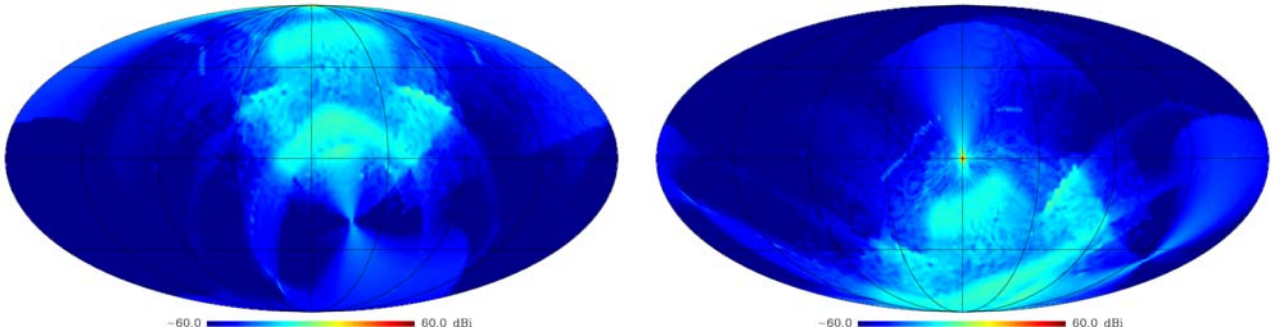

Fig. 4 Full Pattern of the LFI28 SWE X– axis polarized at 30 GHz (power). *Left*: the boresight direction is at the top of the map; *Right*: the boresight direction is in the centre of the map.

3.2.2 Y– polarized

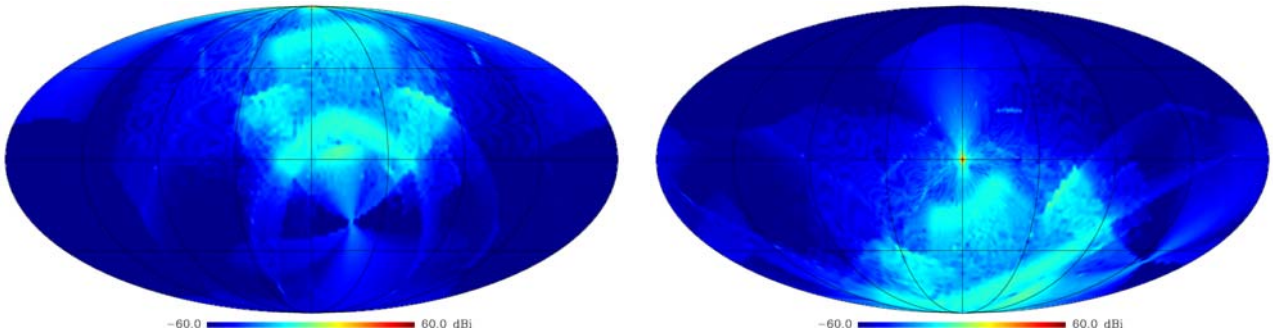

Fig. 5 Full Pattern of the LFI28 SWE Y– axis polarized at 30 GHz (power). *Left*: the boresight direction is at the top of the map; *Right*: the boresight direction is in the centre of the map.

4 REFERENCES

[1] K. Pontoppidan, *Technical Description of GRASP8*, TICRA, Doc.No.S-894-02, 1999.
[2] P. Nielsen, *Manual for Multi-reflector GTD: an add-on package to GRASP8*, TICRA. Doc.No.S-894-05.
[3] M. Sandri and F. Villa, *PLANCK /LFI Optical Simulations: a study on the full pattern prediction with GRASP8 Multi-Reflector GTD*, Internal Report IASF 342/2002, 2002.
[4] FIRST/PLANCK Project, *PLANCK Telescope Design Specification*, SCI-PT-RS-07024.
[5] M. Sandri and F. Villa, *PLANCK/LFI: Main Beam Locations and Polarization Alignment for the LFI baseline FPU*, PL-LFI-ST-TN-027, 2001.
[6] A. C. Ludwig, *The Definition of Cross Polarization*, IEEE Transactions on Antennas and Propagation, pp.116-119, Jan 1973.
[7] M. Sandri, F. Villa, M. Bersanelli, et al., *Advanced simulation techniques for straylight prediction of high performance mm-wave reflecting telescope,* ESA Conf. Proc. WPP-202, 621, 2002, astro-ph/0304142.
[8] C. Burigana, D. Maino, K. M. Gorski, , et al., A&A, 373, 345, 2001.
[9] C. Burigana, M. Sandri, F. Villa, D. Maino, R. Paladini, C. Baccigalupi, M. Bersanelli, N. Mandolesi, *Trade-off between angular resolution and straylight contamination in CMB anisotropy experiments. Paper II. Straylight evaluation*, submitted to A&A, astro-ph/0303645, 2003.
[10] M. Sandri, F. Villa, R. Nesti, C. Burigana, M. Bersanelli, N. Mandolesi, *Trade-off between angular resolution and straylight contamination in CMB anisotropy experiments. Paper I. Pattern Simulations*, submitted to A&A, 2003.
[11] K. M. Gorski, E. Hivon, B.D. Wandelt, *Proceedings of the MPA/ESO Conference on Evolution of Large-Scale Structure: from Recombination to Garching*, ed. Banday A.J., Sheth R.K., Da Costa L., 37, astro-ph/9812350, 1998.

5 ACKNOWLEDGMENTS

We wish to thank people of the Herschel/Planck Project, ALCATEL Space Industries, and the LFI Consortium that are involved in activities related to optical simulations.
Some of the results in this paper have been derived using the HEALPix [11] (see also the HEALPix home page at http://www.eso.org/science/healpix/).

6 APPENDIX

6.1 Simulation methods

Full pattern simulations have been performed using GRASP8 MrGTD, an advanced GTD method developed by TICRA. It computes GTD fields from any number of reflectors sequentially illuminated starting from a given source. MrGTD is a ray−optical method in which the computational time is frequency independent and produces accurate results in about one week per beam, as it has been verified for the LFI 30 GHz channel comparing the results with those obtained using the Physical Optics approach [7]. The contributions (that are, bundles of rays defined by a sequence of scatterers and by the type of interaction – reflection or diffraction – occurred on each of them) taken into account in the simulations presented, are those which power level is greater than −50 dBi (−100 dB) in at least one point of the map. This threshold level represents the required straylight rejection level in the LFI frequency channel. Lower power levels not produce significant straylight contamination from the diffuse Galactic emission, as reported in [8]. Only the 2nd order optical contributions

have been considered since neglecting the 3rd order interactions involve only few % errors on the straylight evaluation [9] [10]. In this framework, we have not considered reflections or diffractions on the V– groove, as well as higher order contributions, since we expect them at very low levels (less than –100 dB).

The computed contributions for the X– axis polarized feed horns are:

1) feed ⇒ far field
2) feed ⇒ reflection on sub reflector ⇒ far field
3) feed ⇒ reflection on main reflector ⇒ far field
4) feed ⇒ reflection on baffle ⇒ far field
5) feed ⇒ diffraction on sub reflector ⇒ far field
6) feed ⇒ diffraction on main reflector ⇒ far field
7) feed ⇒ diffraction on baffle ⇒ far field
8) feed ⇒ reflection on sub reflector ⇒ diffraction on main reflector ⇒ far field
9) feed ⇒ diffraction on sub reflector ⇒ reflection on main reflector ⇒ far field
10) feed ⇒ diffraction on sub reflector ⇒ diffraction on main reflector ⇒ far field
11) feed ⇒ diffraction on sub reflector ⇒ diffraction on sub reflector ⇒ far field
12) feed ⇒ diffraction on main reflector ⇒ diffraction on main reflector ⇒ far field
13) feed ⇒ reflection on main reflector ⇒ diffraction on main reflector ⇒ far field
14) feed ⇒ diffraction on main reflector ⇒ reflection on main reflector ⇒ far field
15) feed ⇒ diffraction on baffle ⇒ reflection on main reflector ⇒ far field
16) feed ⇒ reflection on baffle ⇒ diffraction on baffle ⇒ far field
17) feed ⇒ diffraction on baffle ⇒ diffraction on main reflector ⇒ far field
18) feed ⇒ diffraction on sub reflector ⇒ diffraction on baffle ⇒ far field
19) feed ⇒ reflection on baffle ⇒ diffraction on sub reflector ⇒ far field
20) feed ⇒ reflection on baffle ⇒ diffraction on main reflector ⇒ far field
21) feed ⇒ reflection on baffle ⇒ reflection on main reflector ⇒ far field
22) feed ⇒ reflection on baffle ⇒ reflection on sub reflector ⇒ far field
23) feed ⇒ diffraction on main reflector ⇒ reflection on baffle ⇒ far field
24) feed ⇒ reflection on sub reflector ⇒ diffraction on baffle
25) feed ⇒ reflection on main reflector ⇒ diffraction on baffle ⇒ far field
26) feed ⇒ diffraction on sub reflector ⇒ reflection on baffle ⇒ far field
27) feed ⇒ diffraction on main reflector ⇒ diffraction on baffle ⇒ far field
28) feed ⇒ reflection on main reflector ⇒ reflection on baffle ⇒ far field
29) feed ⇒ reflection on sub reflector ⇒ reflection on baffle ⇒ far field

The same contributions have been considered for the Y– axis polarized feed horns, and also the latter one:

30) feed ⇒ diffraction on sub reflector ⇒ reflection on sub reflector ⇒ far field

The main beam region of each map has been opportunely replaced with a computation carried out using a PO/PTD analysis in order to avoid caustic artefacts originated by the GTD approach.